General Disclaimer

One or more of the Following Statements may affect this Document

- This document has been reproduced from the best copy furnished by the organizational source. It is being released in the interest of making available as much information as possible.

- This document may contain data, which exceeds the sheet parameters. It was furnished in this condition by the organizational source and is the best copy available.

- This document may contain tone-on-tone or color graphs, charts and/or pictures, which have been reproduced in black and white.

- This document is paginated as submitted by the original source.

- Portions of this document are not fully legible due to the historical nature of some of the material. However, it is the best reproduction available from the original submission.

NASA TECHNICAL MEMORANDUM

NASA TM-73894

NASA TM-73894

AXIAL RESIDUAL STRESSES IN BORON FIBERS

by Donald R. Behrendt
Lewis Research Center
Cleveland, Ohio 44135

TECHNICAL PAPER to be presented at the
Second International Conference on Composite Materials
Toronto, Canada, April 16-20, 1978

AXIAL RESIDUAL STRESSES IN BORON FIBERS

Donald R. Behrendt
Physicist
National Aeronautics and Space Administration
Lewis Research Center
Cleveland, Ohio

Abstract

A method of measuring axial residual stresses in boron fibers is presented. With this method, the axial residual stress distribution as a function of radius is determined from the fiber surface to the core including the average residual stress in the core. Such measurements on boron on tungsten (B/W) fibers show that the residual stresses for 102, 142, 203, and 366 μm (4.0, 5.6, 8.0, and 14.4 mil) diameter fibers are similar, being compressive at the surface [about -900 MN/m^2 (-130 ksi)] and changing monotonically to a region of tensile stress within the boron. At approximately 25 percent of the original radius, the stress reaches a maximum tensile stress of about 860 MN/m^2 (125 ksi) and then decreases to a compressive stress near the tungsten boride core. The average core compressive stress is -1170 MN/m^2 (-170 ksi). Data are presented for 203 μm (8.0 mil) diameter B/W fibers that show annealing above 900° C reduces the residual stresses. A comparison between 102 μm (4.0 mil) diameter B/W and boron on carbon (B/C) show that the residual stresses are similar in the outer regions of the fibers, but that large differences near and in the core are observed. For example, the core stress for the B/W fiber is compressive approximately -1300 MN/m^2 (-190 ksi) whereas for the B/C fibers the core is in tension approximately 97 MN/m^2 (14 ksi). Finally, the effects of these residual stresses on the fracture of boron fibers is discussed.

Introduction

The fact that boron fibers produced by chemical vapor deposition (CVD) exhibit large residual stresses has been known for some time. Faughan has shown that the surfaces of both boron deposited on tungsten (B/W) and boron deposited on carbon (B/C) are stressed in compression and that the borided core of B/W fibers is also in compression (1). These stresses can be as large as one-third of the fiber fracture stress. Because the fibers fail in brittle fractures, their strength is greatly influenced by the residual stresses. The objectives of this work were to measure these residual stresses accurately and determine how they affect the fracture stress. Further, the effects of annealing of the fibers on the residual stress distribution were of interest. To achieve these objectives it was necessary to develop a method of accurately measuring residual stresses in the boron coating and core of B/W and B/C fibers. The method that we developed utilized the fact that the residual stress distribution can be calculated from a knowledge of changes in length of a fiber with surface removal. Faughan used a method employing hot nitric acid to etch away the surface. However, his results showed considerable scatter in the data due to the rapid and nonuniform etching of the tungsten boride core by the acid through radial cracks in the boron. In our method, these undesirable effects were mostly eliminated because the removal of the boron surface was done at room temperature by an electropolishing method.

Using this method, we have measured the residual stress distribution in 102, 142, 203, and 366 μm (4.0, 5.6, 8.0, and 14.4 mil) diameter B/W fibers and in 102 and 142 μm (4.0 and 5.6 mil) B/C fibers from the surface to near the core. Also for the 102 and 203 μm (4.0 and 8.0 mil) B/W and the 102 μm (4.0 mil) B/C fiber we determined the average core stresses. These residual stress distributions provided a basis for understanding the effects of chemical etching on the fracture stress of boron fibers (2). In that study, Smith measured the change in tensile fracture stress as a function of etched diameter of 203 μm (8.0 mil) B/W fibers. He has shown that the primary flaws at the surface limit the as-received fiber strength, that a small amount of etching removes these flaws, and that the strength is then limited by flaws located either in the core or near the core-boron interface. Further etching produces an additional increase in strength due to the residual stresses in the fiber.

Specimen Description

The B/W specimens tested were 102, 142, 203, and 366 μm (4.0, 5.6, 8.0, and 14.4 mil) diameter fibers deposited on a 12.7 μm (0.5 mil) tungsten substrate made by AVCO Specialty Materials Division. The 102 and 142 μm (4.0 and 5.6 mil) B/C fibers were also made by AVCO by depositing boron on a graphite coated carbon fiber. The purpose of the 1.3 μm (0.05 mil) thick pyrolytic graphite is to provide a low-shear strength layer between the boron and the 33 μm (1.3 mil) diameter carbon substrate to prevent the elongating boron layer from breaking the carbon core during boron deposition.

The as-received tensile fracture strengths determined by Smith for these fibers are shown in Table I (2).

In another study, four groups of 203 μm (8.0 mil) B/W fibers were annealed respectively at 915° C and 1030° C in vacuum for 60 minutes and at 900° C and 1260° C in argon for 160 minutes (3). Using some of these annealed fibers, we have determined how the residual stress distribution changes by heating in vacuum and argon.

Experimental Test Apparatus

A dilatometer was designed so that as the surface of the fiber was removed by electropolishing, continuous measurements could be made of the length changes of a boron-fiber specimen. From these axial strains, the axial residual stress distribution could be calculated. Figure 1 is a schematic representation of the dilatometer. The specimen is mounted between an inner and an outer quartz tube. The inner tube is free to slide vertically in teflon bushings within the outer tube. The boron fiber to be tested is cemented with conducting epoxy between the bottom of the outer tube and a sleeve connected to the inner tube. Normally, the fiber test section is about 1 cm long. The center plate of a three-plate capacitor is attached to the top of the inner tube. The other two plates are insulated from each other and attached to the top of the outer tube. Thus any change in length of the specimen produce an equal change in the position of the center plate with respect to the outer plates. The relative position of the center plate is detected by applying a 100 volt peak-to-peak 3000 Hz voltage to the outer plates. The resulting signal from the center plate is applied to a high-impedance (10 mΩ) input of a lock-in amplifier. A strip chart recorder provides a continuous recording versus time of the output of the lock-in amplifier. Calibration showed that the position of the recorder pen was linearly related to the position of the center plate of the dilatometer. During the determination, the surface of the boron is removed by electropolishing at room temperature by placing the lower portion of the apparatus in a low-conductivity solution made by dissolving 0.5 g of sodium hydroxide (NaOH) in 30 cm^3 of water and adding this to 150 cm^3 of glycerin. In preliminary tests, it was established that the rate of mass removal from the fiber is constant for given current and independent of fiber diameter. Because the mass removal rate is constant, the fiber diameter could be calculated to an accuracy of 3 percent for any time during the run by knowing the final diameter and the time since start of electropolishing. This allowed the apparatus to remain undisturbed during an actual run since it was not necessary to make physical diameter measurements of the fibers. A complete discussion of this method is given in reference 4.

The advantages of using electropolishing instead of chemical etching are: (1) the electropolishing can be done at room temperature, whereas the chemical etching of boron required etchant temperatures near 100° C to obtain reasonable etching rates and (2) the electropolishing method produces a more uniform removal of the surface. A scanning electron microscope was used to examine the surfaces of the as-received boron fibers and fibers which were either lightly electropolished or chemically etched using a mixture of two parts nitric acid to one part water at 100° C. The as-received fibers had the usual nodular or "ear of corn" appearance. After reducing the diameter by 13 μm (0.5 mil) by electropolishing, the surface was smooth with little evidence of the nodules left. In contrast, the nitric acid-etched surfaces, after removal of a similar amount, were considerably rougher than those produced by electropolishing with the nodular structure clearly evident.

Analysis of Data

The axial strain, ϵ_z, at a given time during electropolishing is calculated from the measurements of changes in fiber length. The radius, r, for the same time during electropolishing is calculated from the final diameter and the time at the end of electropolishing along with the constant rate of mass removal from the fiber during electropolishing. For the purposes of calculating the residual stresses, the mechanical properties of the boron are assumed to be independent of radius; namely, that both the Young's modulus, E, and Poisson's ratio, ν, are constant in the boron. However, for the

core material, the values for E and ν may be different from that of the boron. It is also assumed that the axial strains are produced only by axial stresses. This means that we have neglected the effects of the nonaxial σ_r and σ_θ stresses on the axial strain, ϵ_z. It is not possible to estimate the error introduced by neglecting these terms in the general case since we do not know σ_r and σ_θ. However, in a case in which σ_r, σ_θ, and σ_z were calculated from a simple model, which treats the boron and the core as elastic materials, we determined that the axial stress, σ_z, calculated by neglecting σ_r and σ_θ is overestimated by about 13 percent (4). In the actual case in which the creep of these materials can take place, one might expect a similar error. In our calculation of the residual stresses, no account was taken of this error.

From the data of the axial strain, ϵ_z versus the electropolished radius, r, it is possible to reconstruct the residual stress distribution in the original fiber of initial radius r_o. The stress, $\sigma(r_o,r)$, at radius r of the original fiber of radius r_o can be related to the axial strain, ϵ_z, produced by electropolishing to a radius r by (4).

$$\sigma(r_o,r) = -\left[(E_c - E_b)\frac{r_c^2}{r^2} + E_b\right] \cdot \left[\frac{r}{2}\frac{d\epsilon_z(r)}{dr} + \epsilon_z(r)\right] \qquad (1)$$

where

E_c Young's modulus of the core

E_b Young's modulus of the boron sheath

r_c radius of the core

r radius of the electropolished fiber and also the radius in the original fiber for which the residual stress is determined

$\epsilon_z(r)$ measured axial strain at a fiber radius r with $\epsilon_z(r_o) = 0$

DiCarlo has shown that the core of the 203 μm (8 mil) fiber consists of two tungsten borides; a ditungsten pentaboride (W_2B_5) inner core with an approximate diameter at 12.8 μm (0.5 mil) and a tungsten tetraboride (WB_4) outer core with a diameter of 17 μm (0.67 mil) (5). In Table II, we give his results for the average Young's moduli of these core borides and of the boron sheath for B/W fibers. Also given are similar data for the B/C fibers. Because the Young's moduli for the WB_4 and B are nearly the same, a value of 393 GN/m^2 (57×10^6 psi) was used for these two regions in calculating the residual stresses for all B/W fibers.

Experimental Results

Measurements of the axial strain versus electropolished fiber diameter were made using several to as many as 10 samples of each type of fiber. The measurements were continued until either the core was encountered or the fiber broke. For almost all the B/W fibers, the fiber broke before the core was reached probably because of cracks initiated by the large tensile stresses in the region of the boron near the core. For almost all of the 102 μm (4.0 mil) B/C fibers, it was possible to continue the measurements to the pyrolytic graphite layer without the fiber breaking. In contrast, for the 142 μm (5.6 mil) B/C fibers, fiber breakage halted most measurements near 56 μm (2.2 mil). The as-received 142 μm (5.6 mil) B/C fibers showed local variations in diameter; that is, lumps or sections which were 2.5 to 5 μm (0.1 to 0.2 mil) larger in diameter over a length of approxi-

mately 50 μm (2.0 mil). Such lumps have been associated with hot spots observed during deposition due to breakage of the carbon core. The broken carbon core would account for the fiber breakage during electropolishing.

Using the axial strain versus radius data along the moduli data of Table II for the core and boron portions of the fiber, the residual stress versus radius of the fiber could be calculated using equation (1). The calculated residual stress distributions for each type and size of fiber were averaged to produce a single curve. The variation of any point on a curve of a given set from the average was less than ±15 percent. The residual stress at a distance r from the center of the original fiber is shown in figure 2 for 102, 142, 203, and 366 μm (4.0, 5.6, 8.0, and 14.4 mil) B/W. Here we have used the convention that positive stresses are tensile and negative stresses are compressive. To allow easy comparison, the residual stresses are plotted versus the reduced radius r/r_o where r_o is the radius of the original fiber. In one run of each of the 102 μm (4.0 mil) and 203 μm (8.0 mil) runs, it was possible to continue electropolishing up to the core without the fiber breaking. The tungsten boride of the core is removed very slowly by the conditions required to electropolish the boron so that complete removal of the surrounding boron would take place leaving the bare core. In fact, we have used this method to produce bare cores for other studies. Because the electropolishing was stopped at the core, details of how the stress varies inside the core could not be obtained. However, the average stress in the core could be calculated and is shown in figure 2 by the horizontal, dashed portions of the 102 and 203 μm (4.0 and 8.0 mil) fibers. For all the B/W fibers represented in figure 2, the residual stresses are compressive at the surface and changing to tensile at a radius of 0.70 to 0.75 of the original radius.

In figure 3, the residual stress distributions for the 102 and 142 μm (4.0 and 5.6 mil) B/C fibers are shown. For most of 102 μm (4.0 mil) B/C tested, the fibers did not break before reaching the core allowing the average core residual stress to be calculated. In contrast, all of the 142 μm (5.6 mil) B/C broke before reaching the core, as already pointed out, probably due to existing breaks in the carbon core. These stress distributions are similar to those for the B/W, compressive at the surface and becoming tensile near a radius of 0.75 of the original radius. Significant differences in the residual stresses between the B/C and B/W are apparent near and in the core. The residual stresses near the core changes from tensile to compressive and back to a moderate tensile stress in the core of the B/C fibers; this change takes place over a small change of radius. In contrast, the stress for the B/W fibers changes from tensile near the core to large compressive stress in the core.

Turning now to the results of the annealing experiments, stress distributions are shown in figure 4 for the 203 μm (8.0 mil) B/W in the as-received condition, annealed in vacuum at 915° C for 60 minutes, and annealed in vacuum at 1030° C for 60 minutes. These curves show that annealing produced significant reduction in the magnitudes of the residual stresses in the boron sheath. All the annealed fibers broke before reaching the core so that the annealing effects on the core stress could not be determined.

The residual stress distributions for 203 μm (8.0 mil) B/W fibers in the as-received condition and annealed in argon for 160 minutes at 900° C and 1260° C are shown in figure 5. Both annealed curves differ greatly from the as-received curve. The most significant difference is that the surfaces of both argon annealed fibers are in tension a finding in contrast to that for the vacuum annealed fibers which remain in compression.

Discussion of Results

The similarity of the residual stress distributions for the four sizes of B/W fibers shown in figure 2 suggests that either the chemical vapor deposition of boron from BCl_3-H_2 gas mixture always produces this type of stress distribution or that the optimization of the deposition process required to produce strong fibers produces this similarity.

Processes which give rise to these residual stresses in B/W fibers have been discussed in an earlier paper (4). These were: (1) the boron is deposited with a biaxial deposition stress perhaps arising from surface tension or nodule growth effects, (2) the volume increase of the core due to the formation of the tungsten borides, and (3) the difference in the thermal expansion between the boride core and the boron sheath. Processes which contribute to the residual stresses through atomic motion after deposition are annealing of the disorder produced as the boron is deposited, creep, and anelastic deformation (3). These latter processes would tend to relax the residual stresses. The fact that the surface of the completed fiber is in compression indicates that the deposition stress is compressive. Considering only the deposition stress, and assuming the core and sheath to deform only elastically with the same elastic constants, the axial stress of a completed fiber can be obtained from

$$\sigma_z(r) = \sigma_d\left(1 - 2 \ln \frac{r_o}{r}\right) \qquad (2)$$

where

$\sigma_z(r)$ axial stress at a distance r from the fiber's center

σ_d deposition stress

r_o final radius of the fiber

r radius at which the stress is determined

We can determine σ_d in equation (2) since σ_d equals $\sigma_z(r_o)$ when r equals r_o. If we let σ_d equal -1035 MN/m^2 (-150 ksi), a value typical of those measured in this investigation, $\sigma_z(r)$ increases much more rapidly with decreasing r than our measurements indicate. Such large stresses as predicted by equation (2) would be relaxed during deposition at the deposition temperature of 1300° C due to creep in the boron and possibly in the tungsten boride core. However, we should point out that annealing studies made by DiCarlo indicate that the core does not creep up to 1000° C the highest temperature he investigated (3).

The compressive stress in the core of the B/W fibers is most likely a result of the boriding of the tungsten. Boron diffusing into the tungsten expands the tungsten lattice producing both an axial and radial expansion. The radial expansion can be accommodated to some extent by expanding into the region vacated by the diffusing boron. On the other hand, the axial expansion of the core takes place within an already formed boron sheath which restricts the axial expansion producing an axial compressive stress in the core and an axial tensile stress in the boron. This core compressive stress is relatively large, being -1170 MN/m^2 (-170 ksi) for the 203 μm (8.0 mil) B/W and -1330 MN/m^2 (-190 ksi) for the 102 μm (4.0 mil) B/W.

Because our electropolishing method does not remove the tungsten boride core very rapidly, it was possible to remove cores from the boron for other studies. Figure 6 shows a scanning electron micrograph of such a core (mag-

nification ×1000). We note that the original die drawing marks are clearly visible in the borided core showing that the boriding preserves the original tungsten structure, and also that two sections can be seen where the outer surface of the core has split away, as a result of the handling of the fiber in preparation for the SEM. The nature of this fracture surface would indicate that the stresses in the core are not constant and that the surface layer is in axial and/or radial compression. This would indicate that the outer layer of WB_4 reported by DiCarlo was in compression with respect to the inner W_2B_5 (5).

We believe the initial increase in the compressive stress just inside the original surface for these fibers is associated with the well known nodular surface of boron. In work reported in previous publications, this effect was not apparent; but as improvements in our measuring methods were made, this initial increase in the compressive stress in the first one-to-two percent of the fiber radius became apparent (4).

To compare the stress distributions of the B/W and B/C fibers, we have redrawn the curves for the 102 μm (4.0 mil) B/C fibers in figure 7. The curve for the 102 μm (4.0 mil) fibers does not show the initial increase in the compressive stress with decreasing radius as did most of the boron fibers examined. We believe, however, that residual stresses near the surface of these 102 μm (4.0 mil) B/C fibers would show the initial increase in stress if these fibers had been retested using the newer method of stress measurement. The two curves for the B/W and B/C fibers shown in figure 7 are basically similar except near and in their respective cores. The B/W curve shows that a large compressive stress exists in the tungsten boride core; in contrast, the B/C curve shows that a relatively small tensile stress exists in the carbon core. There is little interdiffusion of boron and graphite layer at the core boron interface. Since the CVD of boron produces an elongation of the growing fiber which stresses the core in tension, the final tensile stress in the core of the B/C fibers is limited by the shear strength of the pyrolytic graphite coating modified by the difference in the rate of thermal expansion between the carbon core and the boron sheath. The reason for the large compressive stress in the narrow region just outside the core of the B/C fibers is not known; however, there is some evidence that a small amount of interdiffusion between the boron and pyrolytic graphite does take place. If this alloy has a specific volume sufficiently larger than carbon and boron or if the difference in the rate of thermal expansion between the alloy and the boron and carbon is large enough, a compressive region could be formed. Evidence for a small amount of interdiffusion of the boron and carbon in the 102 μm (4.0 mil) B/C is seen in figure 8, which shows the core of a B/C fiber after the boron was removed by electropolishing. In this scanning electron micrograph (magnification of ×1000), three regions can be seen with diameters of approximately 33, 36, and 38 μm (1.3, 1.4, and 1.5 mil) which correspond approximately to the diameters of the original carbon core, the carbon core coated with pyrolytic graphite, and a region assumed to be caused by interdiffusion between the boron and pyrolytic graphite. We may further conclude that either the original graphite or the interdiffusion was not uniform since pits in the surface can be seen which could result from the removal of the boron from an irregular surface by the electropolishing. After electropolishing, the entire fiber has an appearance as shown by the largest diameter region of figure 8; however, if the fiber is bent sufficiently, the outer two layers split away in a manner shown in this figure indicating that they are somewhat brittle and are not well bonded to each other and to the carbon core.

We now show how the knowledge of the residual stress distributions can help in understanding the fracture of these fibers and how these stresses can be used to improve the fiber's strength. As the diameter of a fiber is

reduced by etching or electropolishing, the fiber initially contracts along its length due to the removal of the outer compressive layers. This contraction adds a compressive stress to all regions of the remaining fiber including the core. Smith has shown through a study of the average fracture stress of as-received and chemically etched 203 μm (8.0 mil) diameter B/W fibers that reducing the diameter by etching increase their fracture strength (2). He has shown that initial light etching removes surface flaws which produce premature fiber fracture. After this initial etch, almost all the flaws which initiate the cracks are located in or near the fiber core (2). Since etching will increase the compressive stress at the location of the flaws causing the fiber failure, it follows that etching of a fiber should increase its strength by an amount equal to the increase in compressive stress.

From Smith's work (2), we can calculate the core stress at fiber fracture. From our electropolishing-strain data, we can calculate how much the core fracture stress increases over the as-received value due to electropolishing. This is shown in figure 9 where we have plotted the core fracture stress calculated from Smith's data and the core fracture stress from our data obtained by adding our calculated increase in core fracture stress to the as-received core fracture stress of 774 GN/m^2 (1122 ksi) (4). The point for the as-received fibers derived from Smith's data falls well below our curve. This is most probably due to the surface flaws which cause the fiber to break at a stress below the fracture stress due to core flaws.

The good agreement shown in figure 9 supports the idea that the increase in fiber strength with etching is due to the residual stress distribution of these fibers. Relatively large increase in fiber fracture strength can be obtained by etching these fibers. For example, Smith reports an average fracture stress of 4.25 GN/m^2 (616 ksi) for the as-received 203 μm (8.0 mil) diameter fibers; and after etching to a diameter of 138 μm (5.45 mil), the average fracture stress has risen to 5.03 GN/m^2 (730 ksi). Part of this increase which raises the fracture stress to 4.57 GN/m^2 (662 ksi) is due to the removal of surface flaws and the remaining increase to 5.03 GN/m^2 (730 ksi) is due to the residual stresses.

Nomenclature

E Young's modulus

E_b Young's modulus of the boron sheath

E_c Young's modulus of the core

r radius

r_c radius of the core

r_o radius of the fiber before etching or electropolishing

ϵ_z axial strain of the fiber

σ_d biaxial deposition stress

σ_r residual stress in the r (radial) direction at a position r in the fiber

σ_θ residual stress in the θ direction at a position r in the fiber

σ_z residual stress in the z (axial) direction at a position r in the fiber

ν Poisson's ratio

References

1. Faughnan, K. A., "Longitudinal Residual Stresses in Boron Filaments," Proceedings of the Twenty-Ninth Annual Conference of the Wide World of Reinforced Plastics, Society of the Plastics Industry, Inc., New York, 1974, pp. 1-10, Section 4-B.

2. Smith, R. J., "Changes in Boron Fiber Strength Due to Surface Removal by Chemical Etching," NASA TN D-8219, National Aeronautics and Space Administration, Cleveland, Ohio, 1976.

3. DiCarlo, J. A., "Techniques for Increasing Boron Fiber Fracture Strain," presented at the One Hundred Sixth Annual Meeting of the American Institute of Mining, Metallurgical, and Petroleum Engineers, Atlanta, Georgia, March 6-10, 1977. Also, NASA TM X-73627, National Aeronautics and Space Administration, Cleveland, Ohio, 1977.

4. Behrendt, D. R., "Longitudinal Residual Stresses in Boron Fibers," Composite Materials: Testing and Design (Fourth Conference), ASTM Special Technical Publication 617, American Society for Testing and Materials, Philadelphia, Pennsylvania (1977), pp. 215-222.

5. DiCarlo, J. A., private communication.

Table I. Tensile Fracture Stresses of the As-Received Fibers

Fiber type	Diameter, μm (mils)	Average fracture stress, MN/m^2 (ksi)	Coefficient of variation, percent
B/W	102 (4.0)	3310 (480)	9.4
B/W	142 (5.6)	2880 (418)	13.5
B/W	203 (8.0)	3590 (521)	23.5
B/C	102 (4.0)	4190 (607)	6.4
B/C	142 (5.6)	4190 (607)	11.2

Table II. Fiber Mechanical Properties

Fiber	Material location	Diameter of material, μm (mils)	Young's modulus, GN/m^2 (10^6 psi)
B/W	W_2B_5 (Core)	12.8 (0.5)	669 (97)
B/W	WB_4 (Core)	17.0 (0.67)	407 (59)
B/W	B (Sheath)	203 (8.0)	393 (57)
B/C	C (Core)	38.1 (1.5)	41 (6)
B/C	B (Sheath)	102 (4.0)	393 (57)

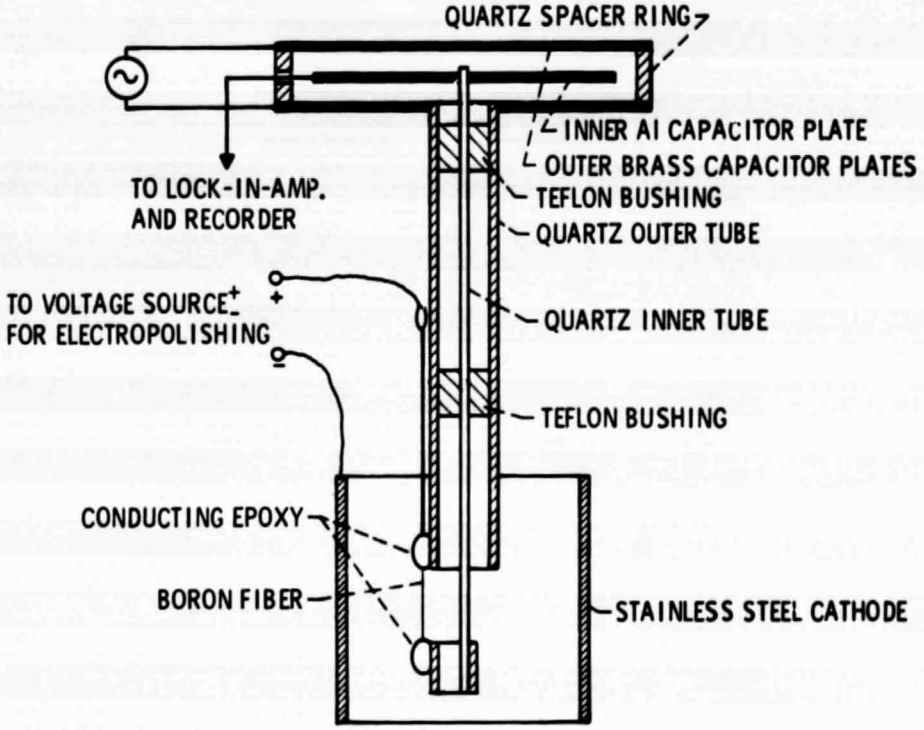

Figure 1. - Dilatometer used to measure length changes of a boron fiber specimen as the fiber's surface was removed by electropolishing.

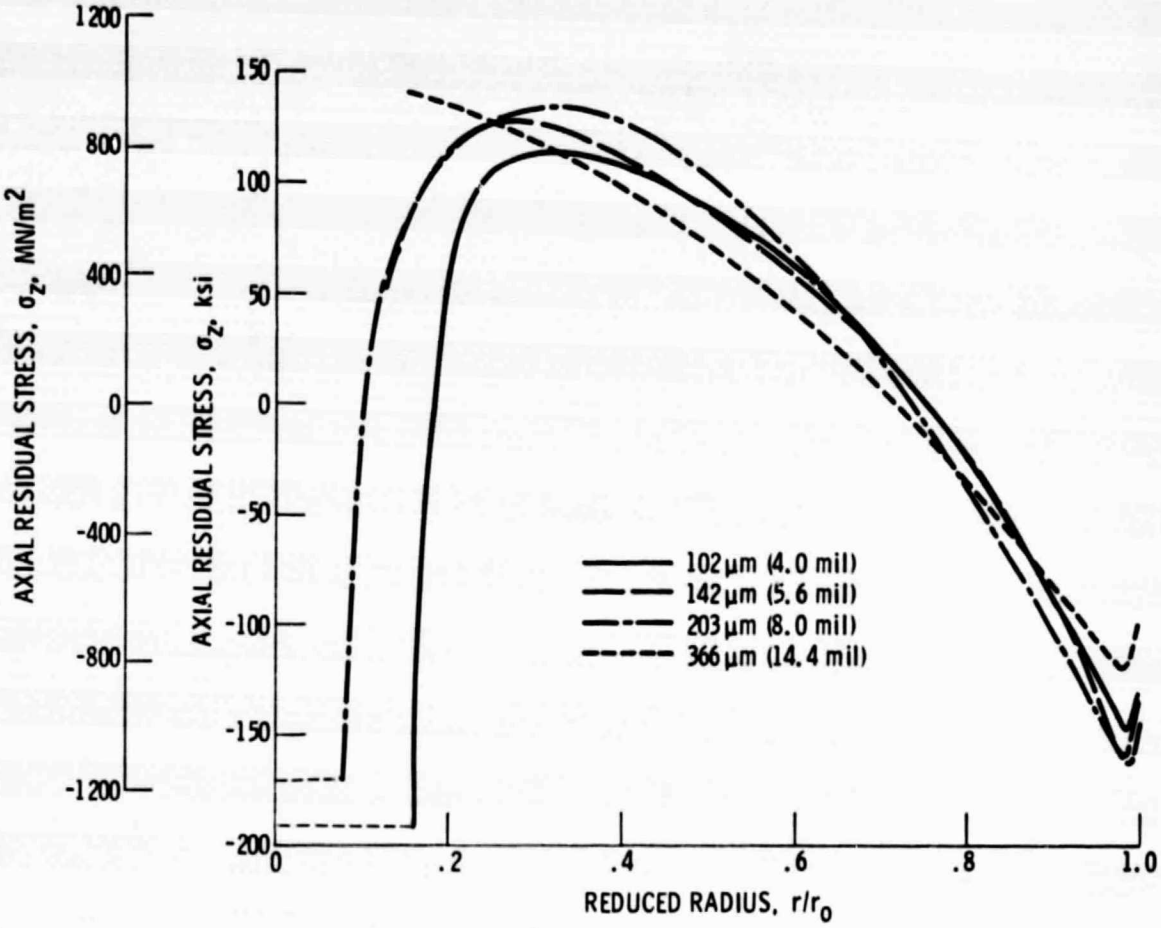

Figure 2. - Axial residual stress distributions for 102, 142, 203, and 366 μm (4.0, 5.6, 8.0, and 14.4 mil) diameter B/W fibers.

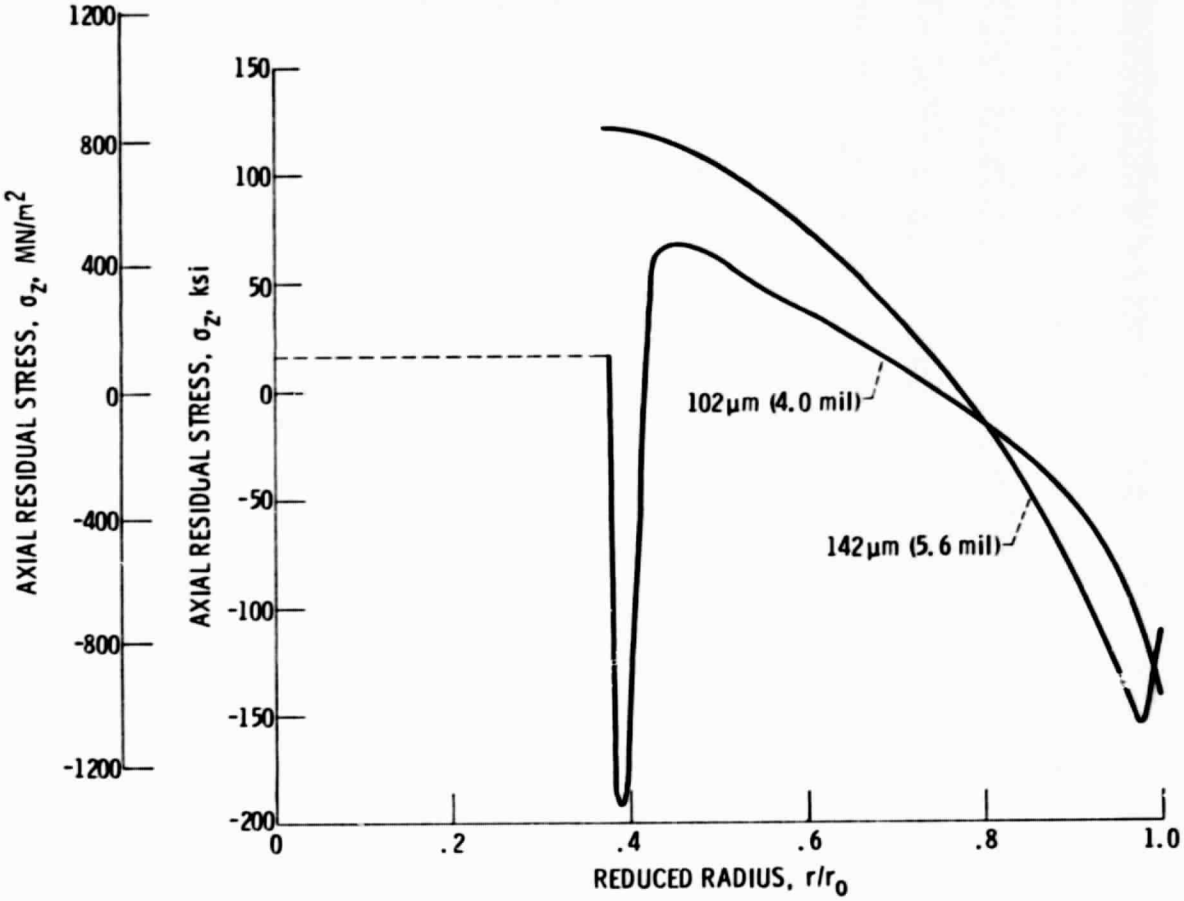

Figure 3. - Axial residual stress distributions for 102 and 142 μm (4.0 and 5.6 mil) diameter B/C fibers.

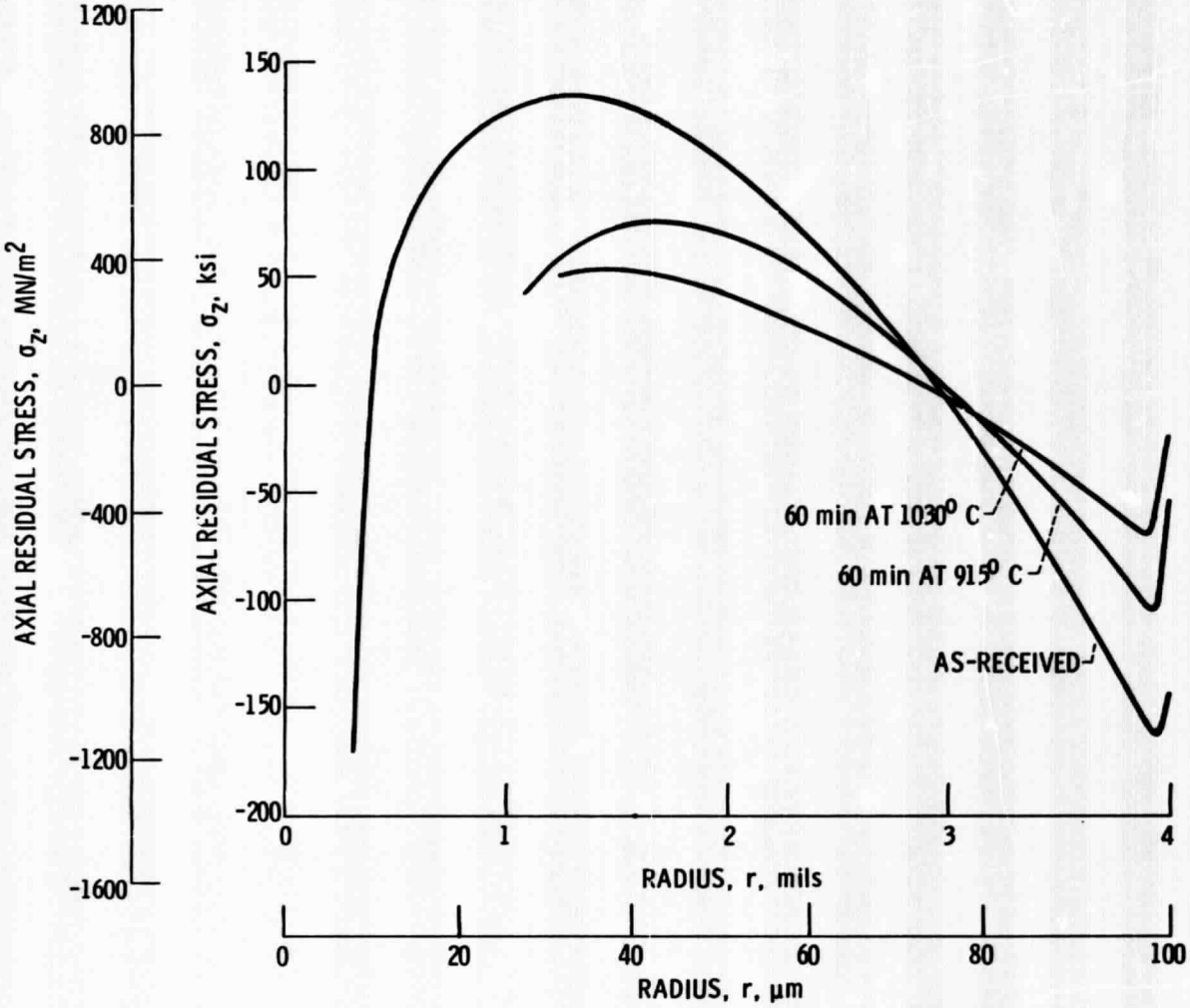

Figure 4. - The effects of annealing in vacuum for 60 minutes on the residual stress distribution of 203 µm (8.0 mil) diameter B/W fibers.

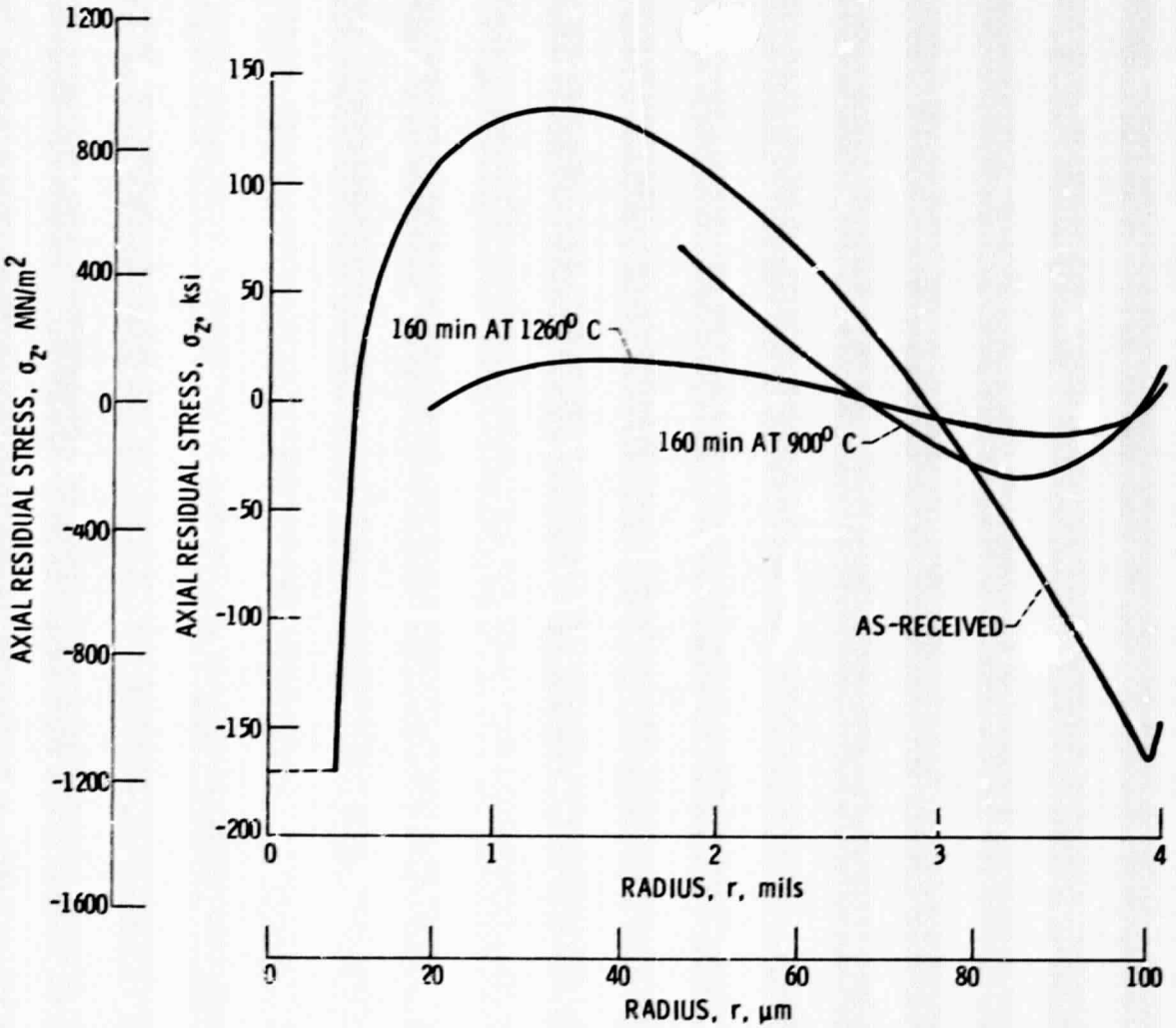

Figure 5. - The effects of annealing in argon for 160 minutes on the residual stress distribution of 203μm (8.0 mil) B/W fibers.

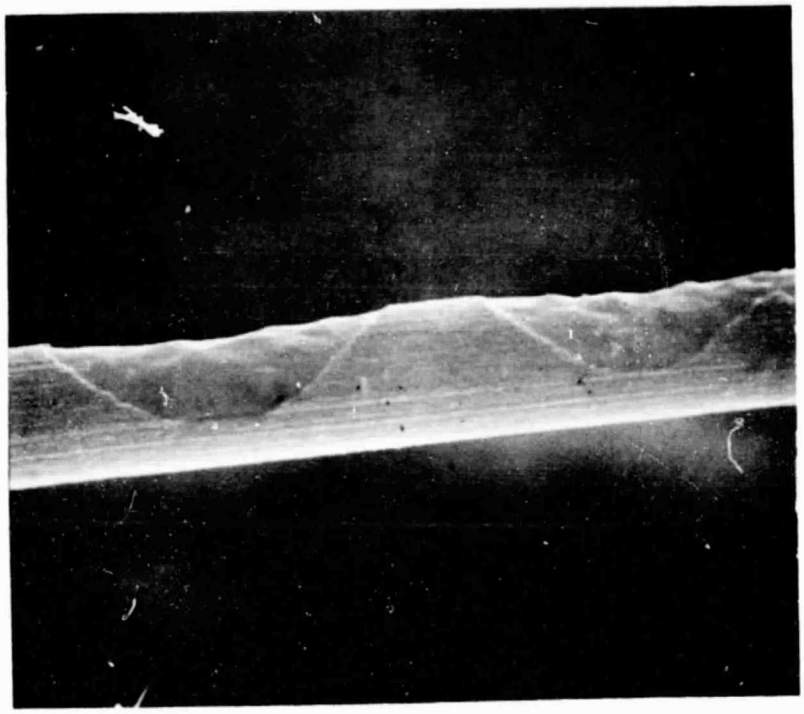

Figure 6. - Scanning electron micrograph of tungsten boride core after complete removal of boron sheath by electropolishing of B/W 102 μm (4 mil) diameter fiber. X1000.

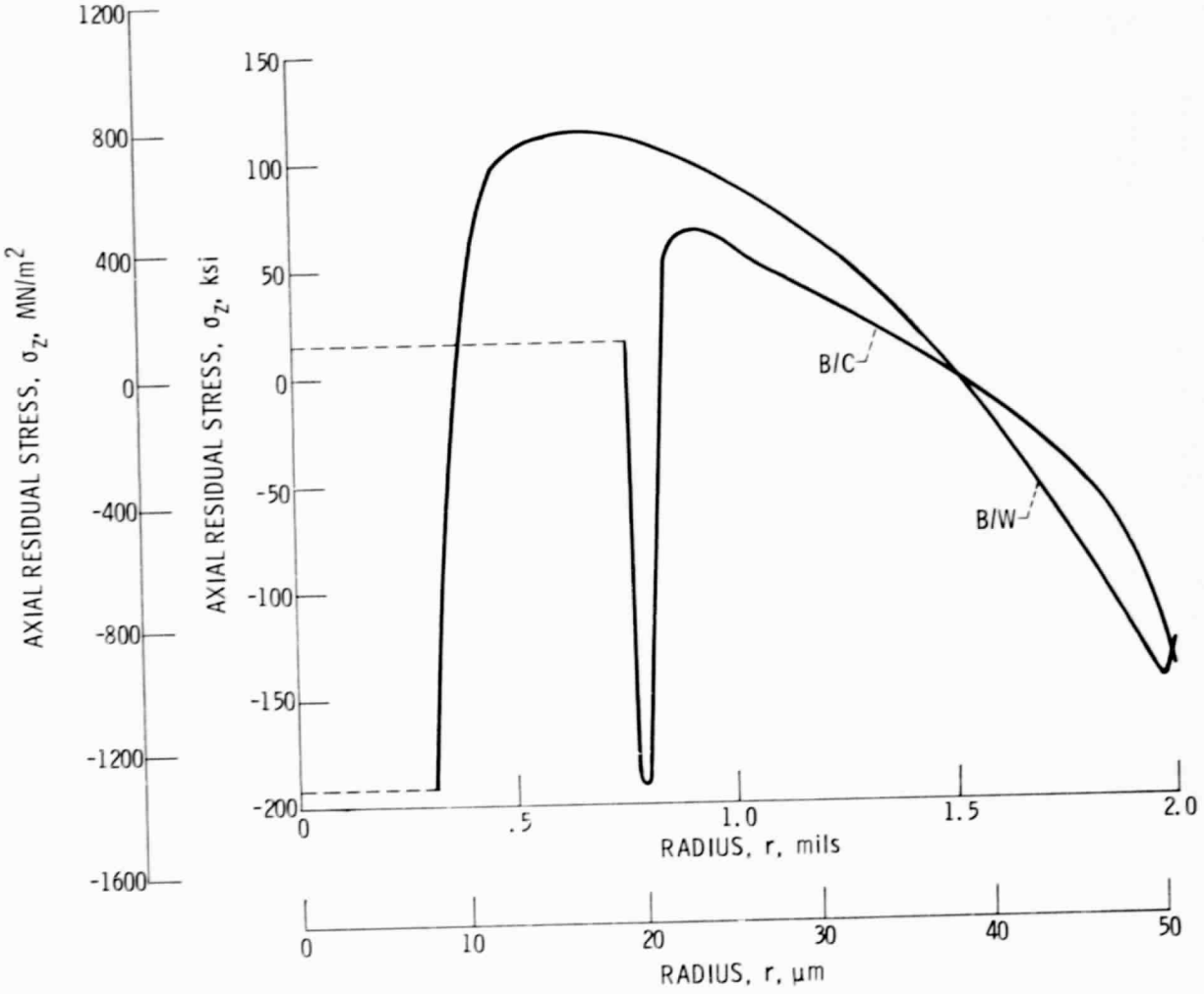

Figure 7. - Axial residual stress distributions for 102 μm (4.0 mil) diameter B/W and B/C fibers.

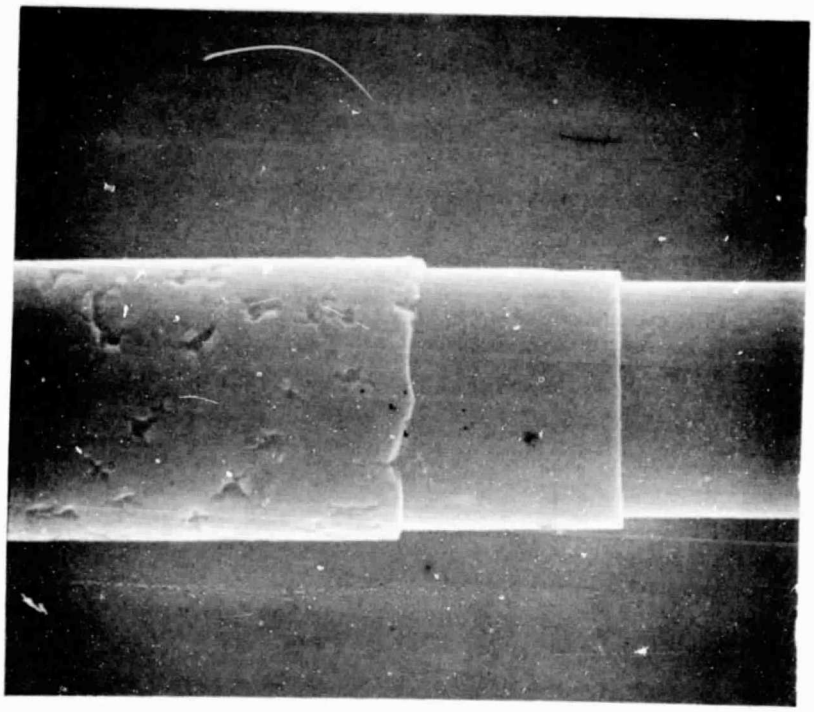

Figure 8. - Scanning electron micrograph of carbon core after complete removal of boron sheath by electropolishing of B/C 102 μm (4 mil) diameter fiber. X1000.

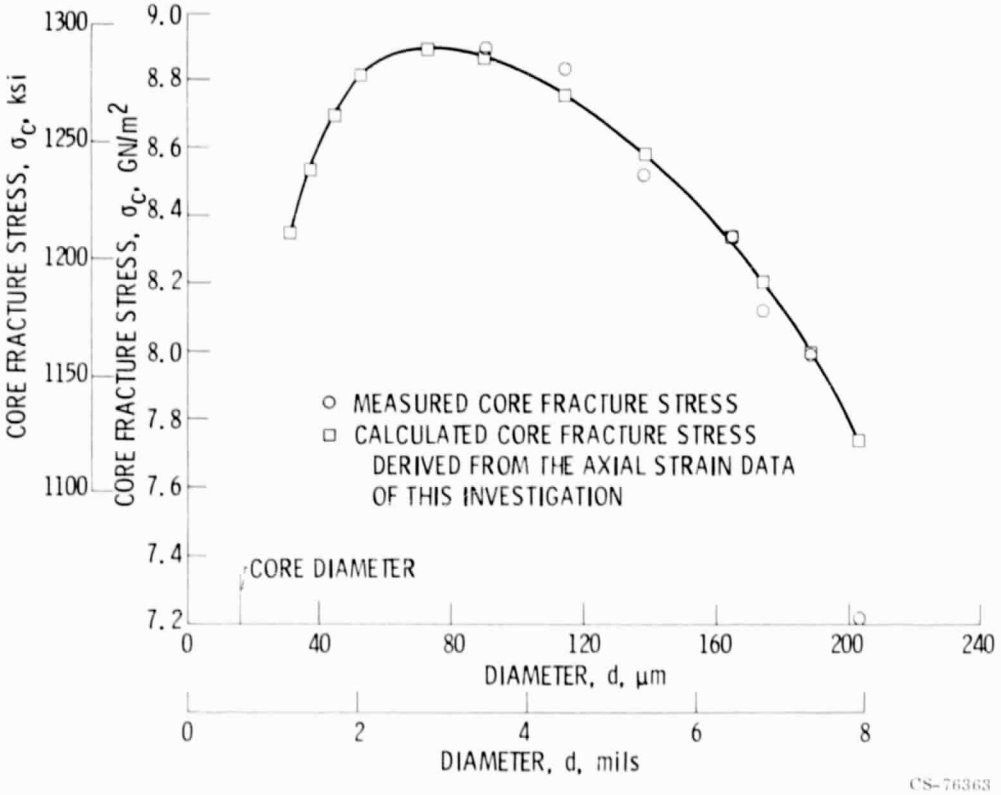

Figure 9. - The dependence of the core fracture stress on the chemically etched diameter of 203 μm (8.0 mil) diameter B/W fibers derived from Smith's work[2] compared with the dependence derived from the axial strain measurements of this investigation.